# Ultrastructural Comparisons of Defective, Partially Defective, and Nondefective Isolates of Impatiens Necrotic Spot Virus

R. H. Lawson, M. M. Dienelt, and H. T. Hsu

U.S. Department of Agriculture, Agricultural Research Service; first author: National Program Staff; second and third authors: U.S. National Arboretum, Floral and Nursery Plants Research Unit, Beltsville, MD 20705.

We thank G. A. Mossman for outstanding technical support and M. Roh for assistance with statistical analysis of immunogold labeling data. We also thank D. Thomas, Goldsmith Seed, Inc., Gilroy, CA, for supplying seedling Impatiens throughout this study.

Accepted for publication 11 March 1996.

## ABSTRACT

Lawson, R. H., Dienelt, M. M., and Hsu, H. T. 1996. Ultrastructural comparisons of defective, partially defective, and nondefective isolates of impatiens necrotic spot virus. Phytopathology 86:650-661.

Cytopathological and serological properties of four isolates of impatiens necrotic spot virus (INSV), Igg, HT-1, HT-2, and B, were compared in infected *Impatiens* 'Accent Salmon.' Igg was a defective form of the virus that failed to form virions but induced extensive networks of paired parallel membranes (PPMs), often in concentric rings. PPMs were continuous with rough endoplasmic reticulum (rER) and the nuclear envelope and were associated with nucleocapsid aggregates (NCAs) and amorphous inclusions (AIs). Infections of HT-1 contained NCAs, AIs, PPMs that included modified Golgi bodies, and virion-like particles within prominent networks of smooth endoplasmic reticulum (sER). Immunogold labeling with polyclonal antibodies to the nucleocapsid protein (N protein) of HT-1 identified the N protein in NCAs and PPMs, including Golgi bodies. Budding at PPMs appeared to form virions, but many particles appeared incomplete, and reactions between particles and HT-1 antiserum were erratic. HT-2 infections contained numerous double-enveloped virions (DEVs) in the cytoplasm, whereas single-enveloped virions (SEVs) were observed within sER and swollen rER cisternae. Polyclonal antiserum to N protein of INSV strongly labeled NCAs and virions. NCAs and masses of SEVs were associated with rER, whereas SEVs within sER were less common. Some DEVs appeared to form at Golgi bodies that labeled inconsistently. Although HT-1 and HT-2 produced virions, differences between these two isolates and INSV B may reflect incomplete replication cycles in the two HT-derived cultures.

The genus *Tospovirus* of the family Bunyaviridae (1) originally was represented only by tomato spotted wilt virus (TSWV), but in 1990, impatiens necrotic spot virus (INSV) was described (12), and by 1993, four additional viruses were recognized (6). Because some tospoviruses have very wide host ranges, it is essential to identify distinguishing properties.

Tospoviruses contain three RNAs that encode six proteins; in addition to nucleocapsid protein (N protein), the proteins include two membrane-associated glycoproteins (G proteins), nonstructural protein (NSs protein), movement protein, and viral polymerase (3,6,11). The replication cycle is complex, incorporating host membranes in viral envelopes and producing distinctive viral inclusions during the course of maturation (5,7,9,10,14,15,20). Tospovirus infections can be distinguished morphologically by the appearance of NSs protein and by the presence or absence of virions. INSV infections contain NSs in arrays of paracrystalline filaments (FIs) (6,12,19,20); in TSWV infections, FIs are parallel or scattered (6,10,11,19,20). Some isolates of TSWV and INSV may be defective and fail to produce virions, but defective TSWV isolates have been identified only after repeated mechanical transmission (8,17,21), whereas defective INSV isolates occur in nature (12,19).

Nondefective isolates produce virions enclosed by a single-unit membrane of host origin and clustered within membranous cisternae associated with the endoplasmic reticulum (ER) (4,5,7,9,10, 14). Double-enveloped virions (DEVs) are present within the cytoplasm; they are thought to represent an early stage of maturation and are generally few in number (5,10,14). Incorporation of two G proteins in the membrane apparently is required for envelopment of the nucleocapsid core (12,17,21). Instead of virions, plants infected with defective isolates primarily contain masses of electron-dense, striated nucleocapsid aggregates (NCAs) (8,13,17, 19,21). NCAs, composed of viral RNA and N protein (5,6,7,13, 14,19,21), usually are not as prominent in mature infections of nondefective tospovirus isolates.

Tospovirus isolates that are partially defective and that produce a range of enveloped and unenveloped virions have not been reported. A variant of INSV that might represent such an intermediate form was subcultured from a defective isolate of INSV (13) isolate Igg from gloxinia (19). The variant, HT-1, produced virions that did not form the multiple clusters characteristic of nondefective tospoviruses. Furthermore, HT-1 failed to produce the striated NCAs characteristic of Igg infections and did not react with a commercial polyclonal antiserum to INSV N protein. HT-1 and a second virion-producing variant, HT-2, were recovered from Igg between the first and fourth serial passage in *Nicotiana benthamiana* plants grown at 27/24°C, light/dark. Infected plants maintained at 21/18°C, light/dark, retained an ultrastructure typical of the defective Igg culture and reacted with the polyclonal INSV antiserum after repeated passage. Here we describe HT-1 and HT-2 in more detail as partially defective isolates and report the distinct serological properties of the N protein of HT-1.

## MATERIALS AND METHODS

**Virus cultures and INSV antiserum.** INSV Igg from gloxinia (19) was used as the defective isolate control. The origins of two variants, HT-1 and HT-2, derived by serial mechanical passage in

Corresponding author: M. M. Dienelt; E-mail address: brannign@asrr.arsusda.gov

Publication no. P-1996-0412-01R

*N. benthamiana* plants grown at high temperature, 27/24°C, light/dark, are shown in Figure 1. INSV B, isolated from *Schizanthus*, served as the nondefective isolate control. All four cultures were maintained in *N. benthamiana*. *Impatiens* 'Accent Salmon' plants were obtained from a commercial source, and the absence of INSV and TSWV was established serologically before use. Polyclonal antiserum to N protein of INSV (Agdia, Elkhart, IN) reacted with Igg, HT-2, and B.

HT-1 N protein was purified from infected *N. benthamiana* plants with a combination of detergent treatment and low-speed centrifugation and separation on a sucrose cushion (H. T. Hsu and R. H. Lawson, *unpublished data*). The resulting supernatant was concentrated at high speed and further separated on a sucrose gradient, followed by equilibrium centrifugation in cesium sulfate. Gradient bands absorbing at 254 nm and containing INSV N protein were collected and sent to Cocalico Biologicals (Reamstown, PA) for production of antisera in rabbits. Antiserum was purified by ammonium sulfate precipitation and was cross-absorbed with sap from noninoculated *N. benthamiana* plants. Antisera to HT-1 reacted in double-antibody sandwich enzyme-linked immunosorbent assay (DAS-ELISA) under standard incubation conditions with HT-1 but not with Igg, HT-2, and B. After protracted overnight incubation, a weak cross-reaction was observed, apparently due to the presence of small amounts of INSV N protein in the immunogen (H. T. Hsu, *unpublished data*).

To ensure that cultures remained true to type and that no cross-contamination occurred, infected plants were monitored throughout the study by testing sap in DAS-ELISA tests against antisera to INSV N protein and to N protein of HT-1.

**Growing environments.** Four to six *Impatiens* plants were inoculated with each of the INSV cultures and placed in growth chambers at 21/18°C, light/dark (LT), and 27/24°C, light/dark (HT), as previously described (13). Tests were performed a minimum of five times with *N. benthamiana* plants infected with the respective isolates as the inoculum source. In two experiments, Igg was sequentially passed through 'Accent Salmon' at HT six times to duplicate the earlier transfers in *N. benthamiana* that yielded HT-1 and HT-2.

**Electron microscopy and immunogold labeling.** Five to seven necrotic local lesions from two to four plants were sampled from LT and HT plants in each series of growth-chamber tests. Samples were fixed in 2% glutaraldehyde and 1.5% acrolein in 0.05 M $Na_2HPO_4$-$KH_2PO_4$ ($PO_4$) buffer, pH 7.0, postfixed in 1% $OsO_4$, dehydrated in a graded series of ethyl alcohol and propylene oxide, and embedded in LX 112 (13). Sections were stained in uranyl acetate and Reynolds lead citrate. When tissue was prepared for immunogold labeling, $OsO_4$ fixation was omitted.

Immunogold labeling was performed with antisera to N protein of HT-1 (7.5 mg/ml) and INSV (Agdia) (1 mg/ml). Plants infected with Igg, HT-1, HT-2, and B and noninoculated controls were evaluated for immunological reactions with cellular inclusions. Sections were mounted on gold grids and treated as previously described (13), except that the concentration of NaCl in the Tris-saline buffer was increased to 0.8 M, and only 10 nm of gold-conjugated goat anti-rabbit antibody (Amersham Life Sciences, Arlington Heights, IL) was used as the secondary antibody. Each test was performed at least three times.

Gold counts on viral inclusions and host structures were determined from electron micrographs of sections of HT-1 incubated with HT-1 antiserum, HT-2 and B incubated with the Agdia antiserum, and noninoculated controls treated with each antiserum. Micrographs of each isolate represented two to three plants from two inoculation dates, three to five immunogold labeling tests, and four to eight sections per test. A Wacom ADB tablet (Vancouver, WA) and pressure-sensitive stylus were used to load outlines of viral inclusions, host structures, and gold particles into a Macintosh II FX computer. Image, an image analysis software in the public domain, determined surface areas and gold counts. The number of gold particles per square $\mu^{-1}$ were calculated and analyzed by the MSTAT-C microcomputer statistical program (Michigan State University, East Lansing). Data were subjected to a one-way analysis of variance, and differences in labeling efficiency were determined by least significant difference (1 SD) at $P < 0.001$. Significance of labeling over background was determined by comparing mean values on Golgi bodies in infected tissue to noninoculated tissue as controls. Mean values on NCAs, virions, paired parallel membranes (PPMs), microbodies, and unidentified inclusions (UIs) were compared to mean values on cytoplasm and cell walls in infected tissue as controls. Only a few gold particles were observed on host structures in inoculated plants, with the exception

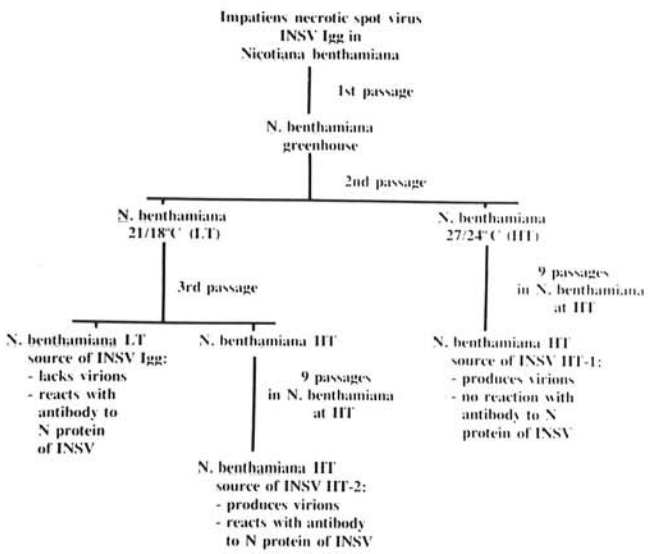


**Fig. 1.** Origin of partially defective impatiens necrotic spot virus (INSV) isolates HT-1 and HT-2 from the fully defective INSV isolate Igg.

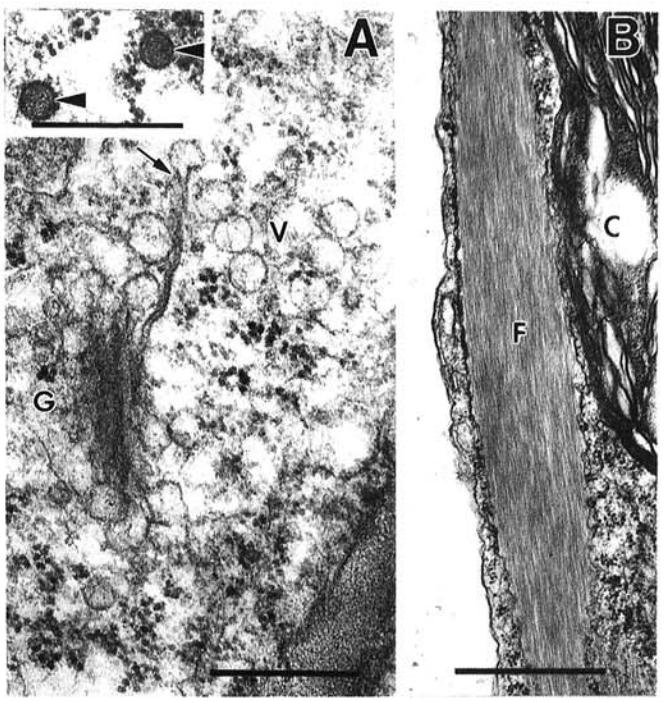


**Fig. 2.** Structures in noninoculated *Impatiens* plants that resembled tospovirus structures. **A,** Vesicles (V) formed at the margins of Golgi (G) cisternal swellings (arrow); some contained electron-dense material (inset, arrowheads) and measured 89 nm in diameter, similar to tospovirus virions. Bar = 330 nm. **B,** Aggregates of filaments (F) resembled tomato spotted wilt virus filamentous inclusions. C = chloroplast. Bar = 800 nm.

of those on Golgi bodies. Therefore, control counts were made, and data was analyzed only from Golgi bodies in noninoculated tissue. Counts on host structures in sections of infected cells were more accurate representations of background for that section specifically.

## RESULTS

**Noninoculated *Impatiens* controls.** Rough ER (rER) was more prevalent than smooth ER (sER); the latter was observed only infrequently, usually next to transfer cell walls in vascular parenchyma cells. Golgi bodies usually consisted of flat or slightly curved stacks of parallel cisternae. Electron-dense material was sometimes observed within cisternae. Golgi vesicles budded from swollen cisternal margins and were enclosed by a single membrane (Fig. 2A), displayed a wide range of sizes and shapes, and were present with and without visible content. Vesicles filled with electron-dense material and measuring 85 to 90 nm in diameter (Fig. 2A, inset) superficially resembled single-enveloped tospovirus particles. Noninoculated plants contained fibrous inclusions, usually in epidermal cells (Fig. 2B). When bounding membranes could not be distinguished, fibers resembled FIs of NSs protein produced by isolates of TSWV.

**INSV Igg.** Elaborate networks of electron-dense double membranes were observed and were often organized in concentric structures containing 10 or more rings (Table 1; Fig. 3A through E). Unit membranes of each pair were parallel to each other, delimited narrow cisternae, and lacked ribosomes over much of their length. In some views, membranes were continuous with rER (Fig. 3A) and nuclear envelopes (Fig. 3B). Concentric membranes were closely associated with nucleocapsid material, and different conformations occurred that appeared to represent different developmental stages (Fig. 3A and C through E). In some infected cells, membranes formed asymmetrical concentric profiles (Fig. 3A) similar to circular rER patterns observed in noninoculated controls; nucleocapsid material was not detected among these membranes. When concentric patterns were more distinct, the cytoplasmic matrix separating each membrane pair sometimes appeared free of viral products (Fig. 3C) but usually contained N protein, either unaggregated and granular (Fig. 3A) or in chainlike NCAs (Table 2; Fig. 3D and E). In sections used for immunolabeling that were not osmicated, double membranes forming concentric rings were not clearly distinguished. As previously reported, however, Agdia INSV N antiserum reacted with aggregated NCAs and more dispersed, granular deposits (13,19). No reactions occurred with antiserum to HT-1.

Increased accumulations of NCAs were associated with poorly organized concentric membrane conformations (Fig. 3E). Unit membranes of each membrane pair appeared to separate, losing their parallel orientation and resulting in cisternae of more irregular diameter (Fig. 3D and E). Membrane separation sequestered cytoplasm and NCAs in regions delineated by single membranes (Fig. 3E) and resulted in cisternal networks resembling sER (Table 1; Fig. 3E).

Amorphous inclusions (AIs) also occurred in areas of membrane proliferation (Table 2; Fig. 3A, B, and E), but unlike NCAs, AIs were not observed between membrane pairs comprising concentric formations. AIs, which do not react with the Agdia INSV antiserum (13,19), were sometimes difficult to distinguish from NCAs in osmicated tissue. Generally, AIs were more electron dense than NCAs and lacked the chainlike configuration and striations characteristic of Igg NCA (19) and other tospoviruses (5,7, 8,10,13). Cytoplasm central to concentric rings often contained homogeneous electron-dense material that lacked striations and resembled small AIs (Fig. 3A and C), but this material could not be clearly identified. Moderately to densely stained globules were often present among AIs and NCAs (Fig. 3E). Although NCAs, AIs, and double membranes often occurred together, double membranes were not always present, and large NCA and AI deposits also were present in cytoplasm that was free of visible membrane proliferation. Paracrystalline FIs, characteristic cytoplasmic features of INSV infections (19,21), were not observed.

When Igg was passaged through six serial mechanical passages in 'Accent Salmon' at HT, virion formation that occurred in similar tests in *N. benthamiana* (13) was not observed. Numerous single-membrane–bounded vesicles measuring 89 nm were present in cytoplasm but did not label with Agdia INSV antibody and could not be distinguished from host vesicles of similar size (Fig. 2A, inset).

**INSV HT-1.** Infections of HT-1 were distinguished by the presence of heterogeneous cytoplasmic accumulations (Fig. 4A through C), virion-like particles (Fig. 4D through F), numerous microbodies (Fig. 4A, D, and E), and prominent PPMs (Fig. 4A). Antibody to N protein of HT-1 localized N protein in electron-dense material at PPMs (Fig. 4A) and in cytoplasmic accumulations (Fig. 4A through C and F; Table 3), identifying the latter as NCAs. NCAs of HT-1 differed from those of Igg, lacking visible striations and regular orientation (Table 2).

Additional cytoplasmic inclusions were present that did not react above background with HT-1 antibody (Fig. 4A through C and F; Tables 2 and 3). Many nonlabeling accumulations displayed gradations in form and staining that made their differentiation difficult; for this reason, we termed them unidentified inclusions. The term amorphous inclusion was reserved for those inclusions with the highly electron dense, compact appearance (Fig. 4B) characteristic of AIs; many AIs, therefore, may have been included in the unidentified category.

Some UIs may represent host components poorly preserved without osmium. In Figure 4A, one of three UIs, UI 1, resembled nearby intact microbodies and, like microbodies, was closely associated with virion-like particles. The association between microbodies and virion-like particles is more clearly shown in the osmicated tissue depicted in Figure 4D and E. Often, UIs were located close to NCAs but were less densely stained (UI 2 in Fig.

TABLE 1. Host endomembrane modifications distinguishing four isolates of impatiens necrotic spot virus in *Impatiens* 'Accent Salmon'[a]

| Isolate | SPM[b] formations | | | | sER proliferation[c] | | rER proliferation[c] |
|---|---|---|---|---|---|---|---|
| | Concentric rER/nucl. exten.[d] | Concentric Golgi bodies[e] | Rings[f] | Curvalinear[e–g] | Rows of virions in tubular cisternae | Nucleocapsids at membranes | Clustered virions in swollen cisternae |
| Igg | ++ | – | – | – | – | + | – |
| HT-1 | – | ++ | + | + | ++ | + | – |
| HT-2 | – | + | + | + | + | + | + |
| B | – | Rare | – | + | + | + | ++ |

[a] – = not observed; + = present; ++ = prominent.
[b] Smooth parallel membrane.
[c] sER = smooth endoplasmic reticulum; rER = rough endoplasmic reticulum.
[d] Nuclear extensions.
[e] Sites of virion formation by budding.
[f] Origin unclear.
[g] Paired parallel membranes characteristic of tospovirus infections.

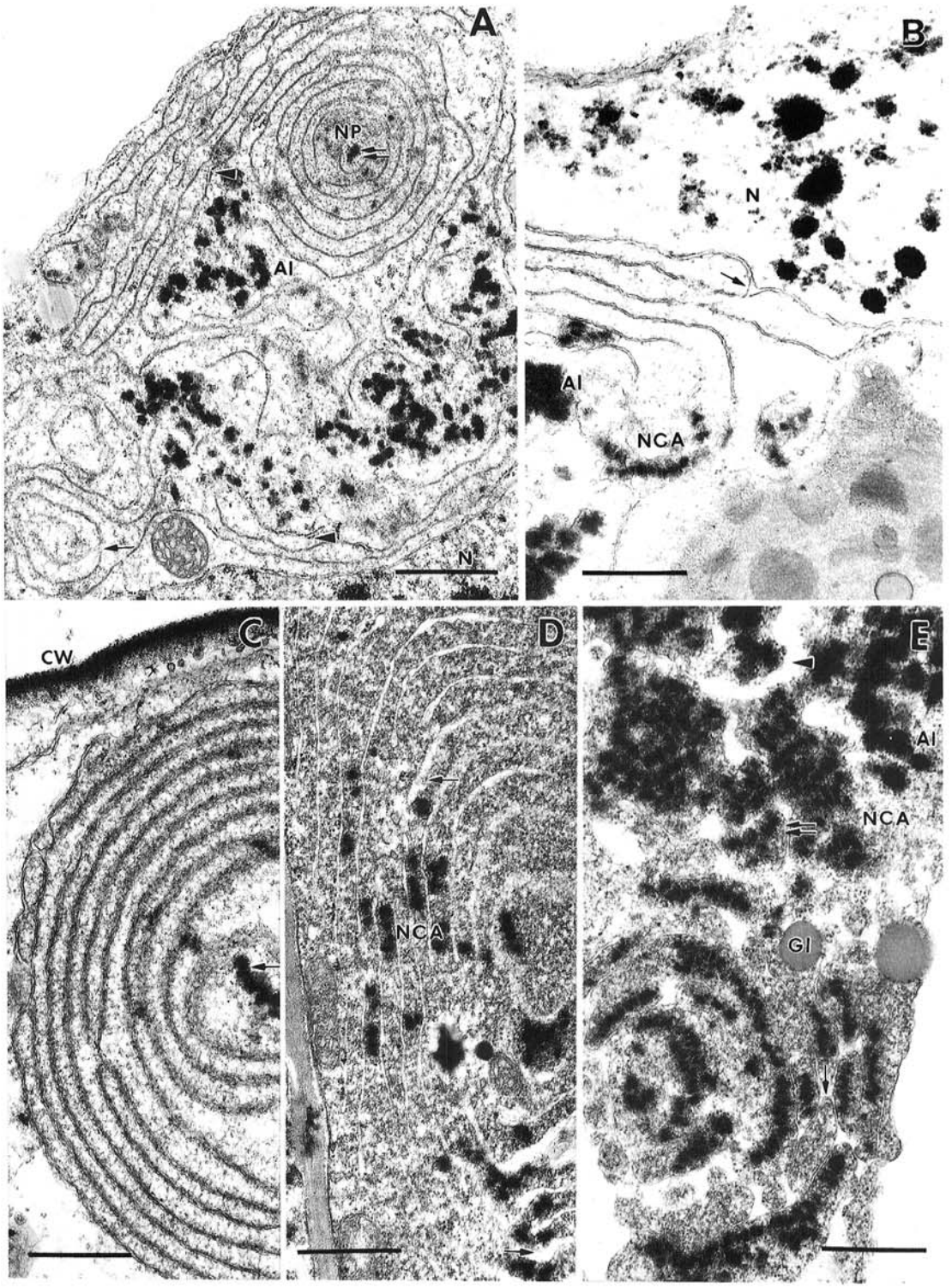


**Fig. 3.** Cytopathology of defective impatiens necrotic spot virus isolate Igg in *Impatiens* 'Accent Salmon.' **A,** Smooth double membranes forming extensive networks, including concentric rings (top center), were more organized than asymmetrical circles of rough endoplasmic reticulum (rER) (lower left, arrow). Ribosomes only lined short segments (arrowheads) of the membranes. Granular nucleocapsid protein (NP) occurred between pairs of double membranes comprising concentric rings. Amorphous inclusions (AI) were near membranes but not between adjacent membrane pairs in concentric formations. Electron-dense material (double arrow) present in the center of concentric rings was not clearly identified as nucleocapsid material or AI. N = nucleus. Bar = 1.2 µm. **B,** Smooth double membranes were continuous (arrow) with the outer membrane of nuclear envelopes. NCA = nucleocapsid aggregates. Bar = 510 nm. **C,** Concentric membranes in a possible early stage of development delimited little or no visible N protein. The central inclusions (arrow) could not be clearly differentiated as NCA or AI. CW = cell wall. Bar = 770 nm. **D,** Concentric membranes in a possible intermediate stage of development delimited N protein condensed into NCA. Double membranes show slight separation (arrows). Bar = 800 nm. **E,** Concentric membranes apparently in a later stage of development had separated, creating pockets of cytoplasm (arrow) and a tubular, smooth ER-like appearance (arrow head). NCA and AI were prominent, with NCA often abutting smooth membranes (double arrow). GI = globose body. Bar = 670 nm.

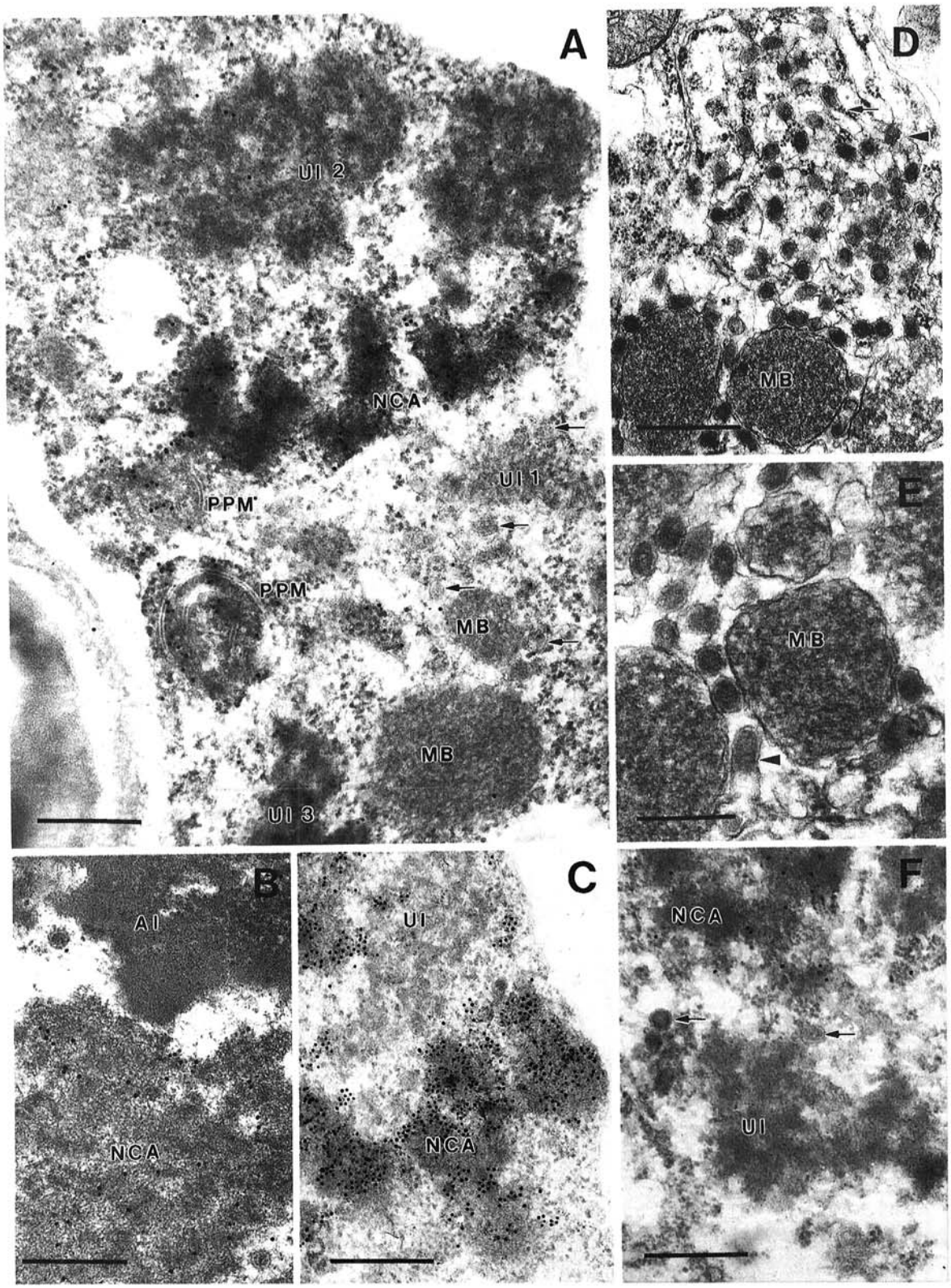


**Fig. 4.** Cytopathology of partially defective impatiens necrotic spot virus isolate HT-1 in *Impatiens* 'Accent Salmon.' **A through C and F,** Immunogold labeled with homologous antiserum to nucleocapsid (N) protein; tissue not osmicated. **D and E,** Tissue osmicated. **A,** N protein was identified in nucleocapsid aggregates (NCA) and at paired parallel membranes (PPM) but not in three unidentified inclusions (UI 1, 2, and 3) or in microbodies (MB). Arrows show faint outlines of virion-like particles. Bar = 250 nm. **B,** Amorphous inclusions (AI) were highly electron dense, and N protein was not detected. Bar = 250 nm. **C,** Some UI were associated with NCA but differed in staining characteristics and immunogenicity. Bar = 420 nm. **D,** Virion-like particles occurred in complex networks of smooth (arrow head) and rough (arrow) endoplasmic reticulum (sER and rER, respectively) and in cisternae surrounding MB. Bar = 510 nm. **E,** Virion-like particles in sER (arrowhead) lacked definite envelopes. Bar = 250 nm. **F,** Most virion-like particles (arrows) failed to react with homologous antiserum. N protein was detected in NCA but not in nearby UI with similar morphological and staining qualities. Bar = 250 nm.

4A, UI in Fig. 4C). Still other UIs were sometimes next to NCAs and displayed staining and morphology similar to NCAs but could only be distinguished from the latter by an absence of labeling (UI 3 in Fig. 4A, UI in Fig. 4F).

Although double- and single-enveloped virions (DEVs and SEVs, respectively) were observed in HT-1 infections, most virions displayed indistinct outer surfaces, as though partially or entirely lacking an envelope (Fig. 4D and E; Table 4). Such virion-like particles were often observed within extensive networks composed of tubular sER and short segments of rER (Fig. 4D). Virion-like particles also were observed in rows within sER surrounding microbodies. Many particles were elongated, but measurements of spherical particles within sER revealed that of 202 virion-like particles ranging from 71 to 344 nm, 22% measured 89 nm in diameter and an equal percent measured 107 nm. Although virion-like particles often displayed low numbers of gold particles in immunogold labeling tests, in many cells particles failed to display any reaction (Fig. 4F). Mean labeling of virions and virion-like particles was not statistically significant from mean labeling efficiencies on cell walls and cytoplasm used as background controls (Table 3).

TABLE 2. Five types of cytoplasmic inclusions used to distinguish four isolates of impatiens necrotic spot virus (INSV) in *Impatiens* 'Accent Salmon'[a]

| Isolate | NCAs[b] | NCAs[c] | UIs[d] | AIs[e] | FIs[f] |
|---|---|---|---|---|---|
| Igg | ++ | – | – | + | – |
| HT-1 | – | ++ | + | + | – |
| HT-2 | + | – | – | + | – |
| B | + | – | – | – | Rare |

[a] – = not observed; + = present; ++ = prominent.
[b] Nucleocapsid aggregates: striated, often with a beaded appearance, reacted with polyclonal INSV antiserum (Agdia) to nucleocapsid (N) protein but not with antiserum to N protein of INSV HT-1.
[c] Nucleocapsid aggregates: lack clear striations and a regular orientation, failed to react with the antiserum but did react with INSV HT-1 antiserum.
[d] Unidentified inclusions: inclusions of variable appearance that failed to label with either antiserum but may contain virions and frequently be in close proximity to NCAs.
[e] Amorphous inclusions: electron-dense, opaque inclusions that failed to react with the Agdia or INSV HT-1 antisera.
[f] Filamentous inclusions: present in infections of Igg, HT-2, and B but not of HT-1 in *Nicotiana benthamiana* plants.

TABLE 3. Mean number of gold particles on host (*Impatiens*) and viral (impatiens necrotic spot virus [INSV] isolates HT-1, HT-2, and B) structures immunogold labeled with antisera to nucleocapsid (N) protein[a]

| | HT-1 antibody[b] | INSV antibody[b] | |
|---|---|---|---|
| Structure | HT-1[c] | HT-2[c] | B[c] |
| Cell walls[d] | 0.08 | 0.09 | 0.15 |
| Cytoplasm[d] | 0.12 | 0.20 | 0.19 |
| Golgi bodies[e] | 1.31[f] | 0.88 | 0.21 |
| NCAs[g] | 1.84[f] | 3.36[f] | 3.49[f] |
| Virions | 0.60 | 1.24[f] | 1.05[f] |
| PPMs[h] | 1.31[f] | 0.66 | 0.72 |
| Microbodies | 0.03 | 0.09 | 0.18 |
| UIs[i] | 0.11 | n/o[j] | n/o |

[a] All data shown is based on the mean number of gold particles per square $\mu^{-1}$ derived from three to five immunogold labeling tests, four to eight sections per test.
[b] Polyclonal antiserum to N protein.
[c] Virus-infected tissue.
[d] Control structures in the cells of infected tissues.
[e] Golgi bodies in noninoculated tissue showed average gold particle counts of 0.04 and 0.10 with HT-1 and INSV antibodies, respectively.
[f] Labeling efficiency of these structures was significantly different from the controls (cell walls and cytoplasm in infected cells and Golgi bodies in noninoculated tissue).
[g] Nucleocapsid aggregates.
[h] Paired parallel membranes.
[i] Unidentified inclusions.
[j] Not observed.

PPMs in HT-1 infections were variable in appearance and were associated with electron-dense material (Fig. 5A through J) and budding profiles (Fig. 5A and C through F). Golgi bodies resembled PPMs and often contained concentric cisternae (Fig. 5A and B). Budding appeared to take place through Golgi cisternae, (Fig. 5C and D) or at cisternal margins (Fig. 5E and F). PPMs also appeared as elongated curvalinear forms (Fig. 5G and H) and as rings of variable size and content (Fig. 5I and J). Smaller rings with electron-dense cores resembled DEVs, whereas larger rings were similar to circular cisternae of Golgi bodies. Immunogold labeling identified N protein in electron-dense material massed at PPMs and Golgi bodies, with labeling efficiencies significantly higher than those of background controls, and on Golgi bodies from noninoculated plants. (Table 3; Fig. 5B, D, F, H, and J).

**INSV HT-2.** Most Golgi bodies in HT-2 infections resembled the flattened cisternae present in noninoculated plants. Budding profiles were similar to those in HT-1 infections, with hooklike structures at the margins of the membranes (Fig. 6A) and rounded swellings through the central portion of the membrane (Fig. 6B). Unlike HT-1 infections, electron-dense material did not accumulate in masses around the membranes. Gold label was observed at these sites (Fig. 6C) but was not significantly different from controls (Table 3). Partially enveloped virion-like structures, such as those thought to represent nucleocapsids budding through flattened Golgi vesicles (10), also were observed (Fig. 6D).

DEVs were abundant in the cytoplasm (Table 4; Fig. 6E), and many sections lacked SEVs entirely. Of 235 spherical virions measured from three inoculations, 132 (56%) were DEVs. Diameters of DEVs ranged from 64 to 196 nm, with 15% measuring 125 nm, 13% measuring 143 nm, and nearly 11% measuring 107 nm.

Many DEVs contained moderately stained fibrillar cores that appeared less compact than cores of HT-1 virions (Table 4; Fig. 6A and E). Fibrillar, rather than electron-dense cores were observed apparently budding through Golgi membranes (Fig. 6A). Structures also were observed among DEVs that appeared to represent incomplete, possibly degenerating forms, including elliptical virion-like particles enveloped by double membranes but with cores diffuse or absent (Fig. 6E), detached envelope-like membranes (Fig. 6D), electron-dense cores with only a single envelope (Fig. 6D and E), and asymmetrical single-membrane–bounded vesicles with fibrillar content (Fig. 6B and D).

Virions were often connected to sER and to each other by narrow constrictions in outer membranes (Fig. 6F), and tubules of sER contained rows of spherical and elliptical SEVs. It was not clear whether DEVs were fusing to or SEVs were budding from the sER. Because it was not always possible to determine when the smooth membrane was part of the cisternal membrane and when it was an outer viral envelope, distinctions between DEVs and SEVs could not always be resolved. In nonosmicated tissue used in immunogold labeling tests, sER membranes were often not visible, but spherical and elliptical virions in rows or as solitary units may represent DEVs or SEVs within sER (Fig. 6G). Im-

TABLE 4. Morphology of virions and virion-like particles produced by four isolates of impatiens necrotic spot virus in *Impatiens* 'Accent Salmon'[a]

| Isolate | SEVs clustered in rER[b] | SEVs in sER[b] | DEVs in cytoplasm[c] | One envelope unclear[d] | Diffuse fibrillar cores[d] |
|---|---|---|---|---|---|
| Igg | – | – | – | – | – |
| HT-1 | – | + | + | ++ | + |
| HT-2 | + | + | ++ | + | ++ |
| B | ++ | + | + | – | Rare |

[a] – = not observed; + = present; ++ = prominent.
[b] SEVs = single-enveloped virions; rER = rough endoplasmic reticulum; sER = smooth endoplasmic reticulum.
[c] DEVs = double-enveloped virions.
[d] Abnormal.

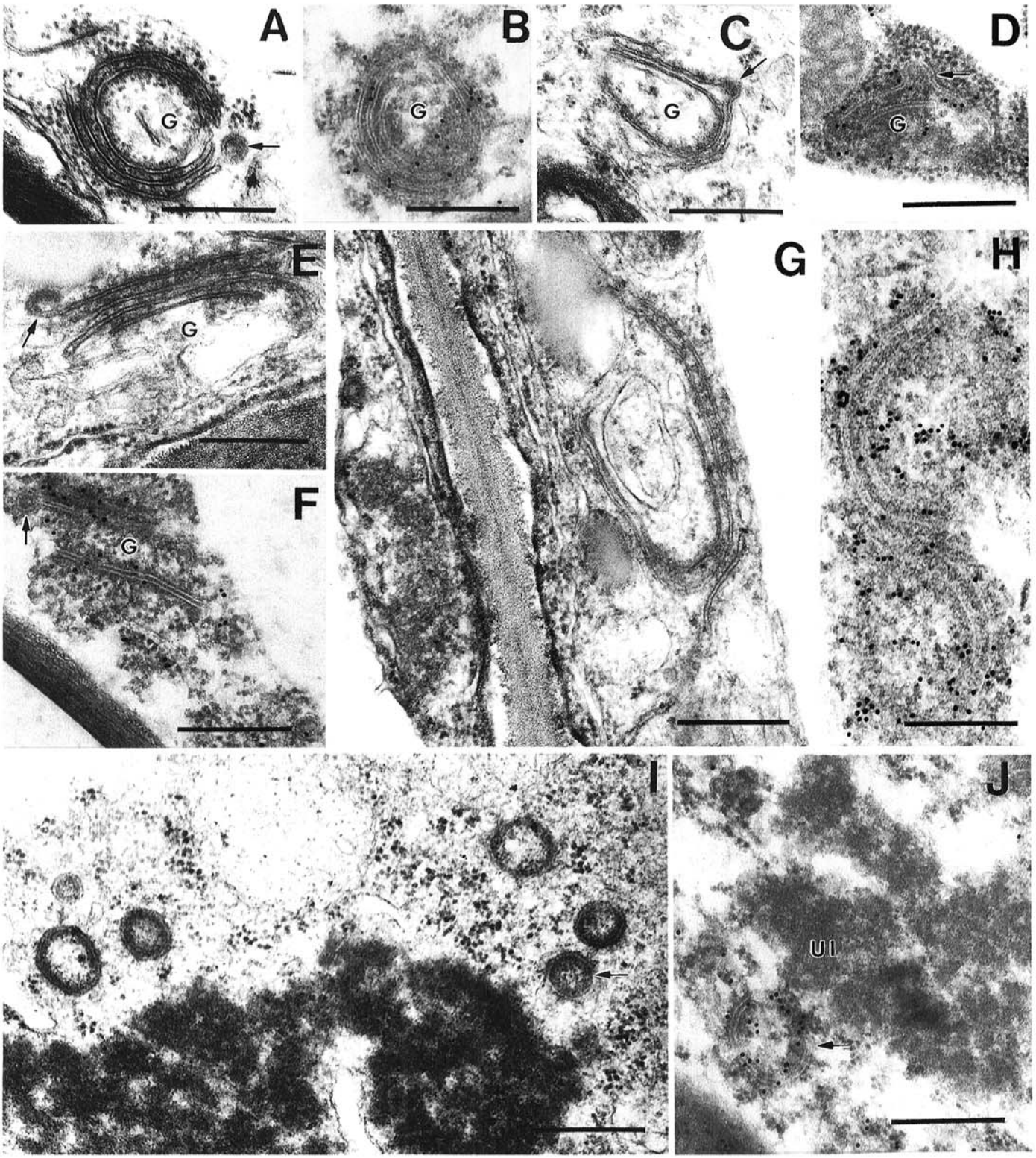


**Fig. 5.** Morphology and immunogenicity of parallel membranes produced in impatiens necrotic spot virus isolate HT-1 infections in *Impatiens* 'Accent Salmon.' **A through F,** Golgi bodies (G); **G and H,** curvalinear forms; and **I and J,** double membrane rings. Images of osmicated structures alternate with images of similar structures immunogold labeled with homologous antiserum to nucleocapsid (N) protein. Arrows in **A and C through F,** budding that may be associated with virion formation; arrow in **J,** immFnogold-labeled membrane ring next to unidentified inclusions (UI) lacking label. **A and E,** Bars = 310 nm; **B, D, F, G, and J,** bars = 250 nm; **C and I,** bars = 400 nm; and **H,** bar = 190 nm.

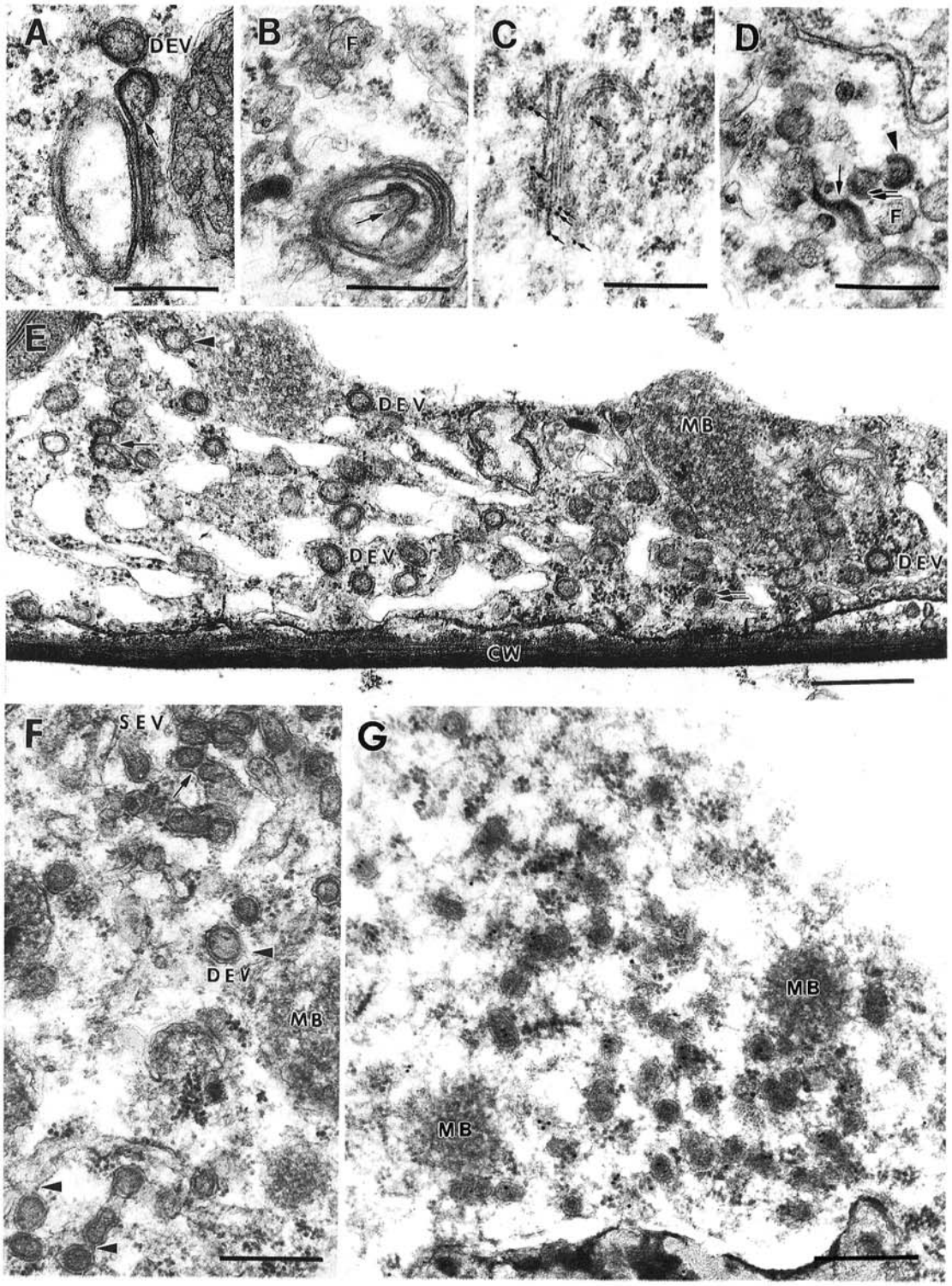


**Fig. 6.** Cytopathology of partially defective impatiens necrotic spot (INSV) isolate HT-2 in *Impatiens* 'Accent Salmon.' **A,** Double-enveloped virions (DEV) often contained diffuse fibrillar cores that were present from initial budding (arrow) at cisternal margins of Golgi bodies. Bar = 330 nm. **B,** Budding (arrow) also occurred through Golgi cisternae. F = fibrillar vesicles. Bar = 330 nm. **C,** Immunogold labeling with antibody to nucleocapsid (N) protein of INSV yielded sparse numbers of Au (arrows) at Golgi bodies. Bar = 250 nm. **D,** Structures possibly associated with incomplete virions included budding profiles through flattened vesicles (arrow head), detached envelope-like membranes (arrow), fibrillar vesicles (F), and virion-like particles with single envelopes (double arrow). Bar = 330 nm. **E,** DEV were prominent, many with elliptical forms (arrow) and diffuse or empty cores (arrow head). MB = microbody; CW = cell wall; and double arrows indicate virion-like particles with single envelopes. Bar = 420 nm. **F,** Many DEV were connected to smooth endoplasmic reticulum (sER) and to each other by constrictions in cisternal membranes (arrow heads). Single-enveloped virions (SEV) within sER-like cisternae (arrow) also were present. Bar = 310 nm. **G,** Virions, which appear to be DEV or rows of SEV in sER, gave erratic reactions to immunogold labeling tests with antiserum to INSV N protein. Bar = 300 nm.

munogold labeling of such virions was inconsistent, with many particles remaining unlabeled (Fig. 6G).

SEVs occasionally were associated with the rER, appearing as clusters within swollen rER cisternae and as solitary virions in the terminus of rER strands (Fig. 7A). Diameters of clustered SEVs were 63 to 143 nm, with about 40% measuring 89.3 nm and 10% measuring 106 nm. Many cells displayed large prominent networks of sER even when few virions were present (Table 1; Fig. 7B). NCAs often accumulated within areas of sER proliferation and were adjacent to sER membranes. Both NCAs and clustered SEVs were significantly labeled above background by the Agdia INSV antibody (Fig. 7C; Table 3).

AIs were observed infrequently, whereas FIs did not appear to be present (Table 2). Microbodies prominent in HT-1 infections were also common in HT-2 infections. No differences were observed in the cytopathology of HT and LT plants. Immunogold labeling confirmed ELISA results, showing no reaction between HT-2 and HT-1 antiserum.

**INSV B.** INSV B produced virus inclusions characteristic of many nondefective tospovirus isolates. Of 397 virions measured, 376 were SEVs. Their diameters ranged from 66 to 141 nm, with 37% measuring 89.3 nm and about 17% measuring 106 nm. Although some swollen, empty particles were present, most cores appeared moderately to densely stained and compact (Table 4; Fig. 8A).

SEVs were observed primarily within swollen cisternae delimited by membranes lined with ribosomes. Cisternae were often associated with the rER, either as swollen extensions of an rER terminus or connected along the rER strand by a narrow membrane bridge (Table 1; Fig. 8A). There was extensive proliferation of sER that seemed to be continuous with rER in some regions and associated with vesicles and DEVs in others. Rows of SEVs within sER were observed infrequently.

Striated NCAs were present in cytoplasm between sER segments (Fig. 8A) and were labeled significantly above background with Agdia INSV antibody (Table 3; Fig. 8B). Golgi bodies were observed that appeared to be involved in virion formation (Fig. 8A, inset), but labeling of Golgi bodies was inconsistent (Fig. 8C) and not statistically significant. Of 48 Golgi bodies analyzed, 22 had associated gold particles and 26 did not. AIs were not observed, and paracrystalline FIs were observed in only two samples (Table 2). Microbodies present among virions in HT-1 and HT-2 infections were common. No differences were observed between LT and HT plants.

## DISCUSSION

Although INSV HT-1, HT-2, and B formed virions and are by definition nondefective, HT-1 and HT-2 produced abnormal virions and are more accurately termed partially defective. Each isolate induced unique cytopathological changes and could be distinguished by several features, including morphology of virions, serology and structure of nucleocapsid material, effect on host membranes, and the presence or absence of cytoplasmic inclusions such as AIs or FIs.

INSV Igg was the only isolate that induced extensive formation of smooth double membranes but failed to produce virions. Double membranes were indistinguishable from PPMs characteristic of

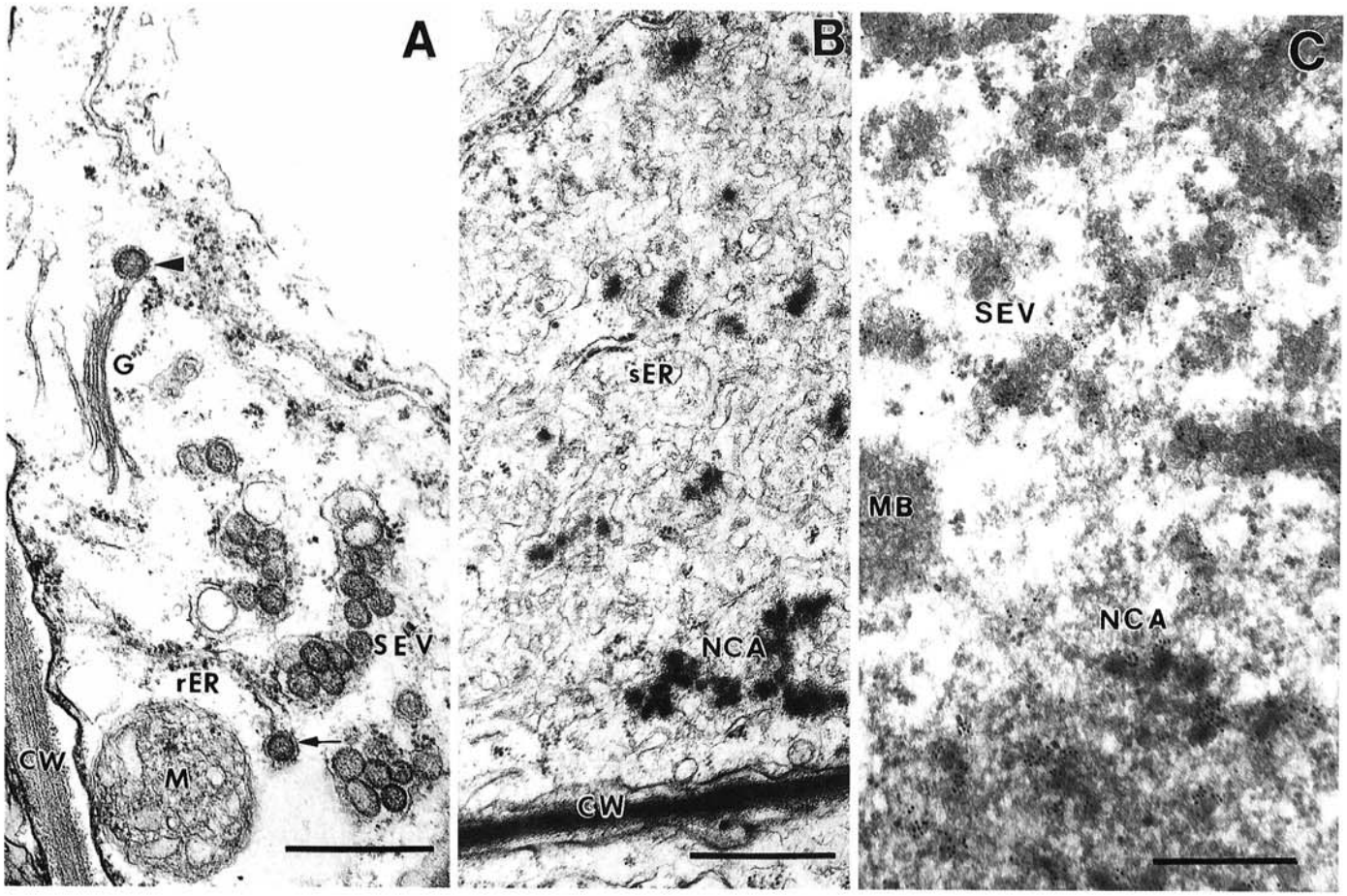


**Fig. 7.** Cytopathology of partially defective impatiens necrotic spot virus (INSV) isolate HT-2 in *Impatiens* 'Accent Salmon.' **A,** Mature single-enveloped virions (SEV) were clustered within swollen rough endoplasmic reticulum (rER) cisternae or present as single bodies at the terminus (arrow) of the rER. The double-enveloped virions (DEV; arrowhead) appeared to have originated from the nearby Golgi body (G). M = mitochondrion; CW = cell wall. Bar = 400 nm. **B,** Nucleocapsid aggregates (NCA) were associated with prominent smooth ER (sER). Bar = 670 nm. **C,** NCA and clustered SEV reacted with antibody to INSV nucleocapsid (N) protein in immunogold labeling tests. Bar = 375 nm.

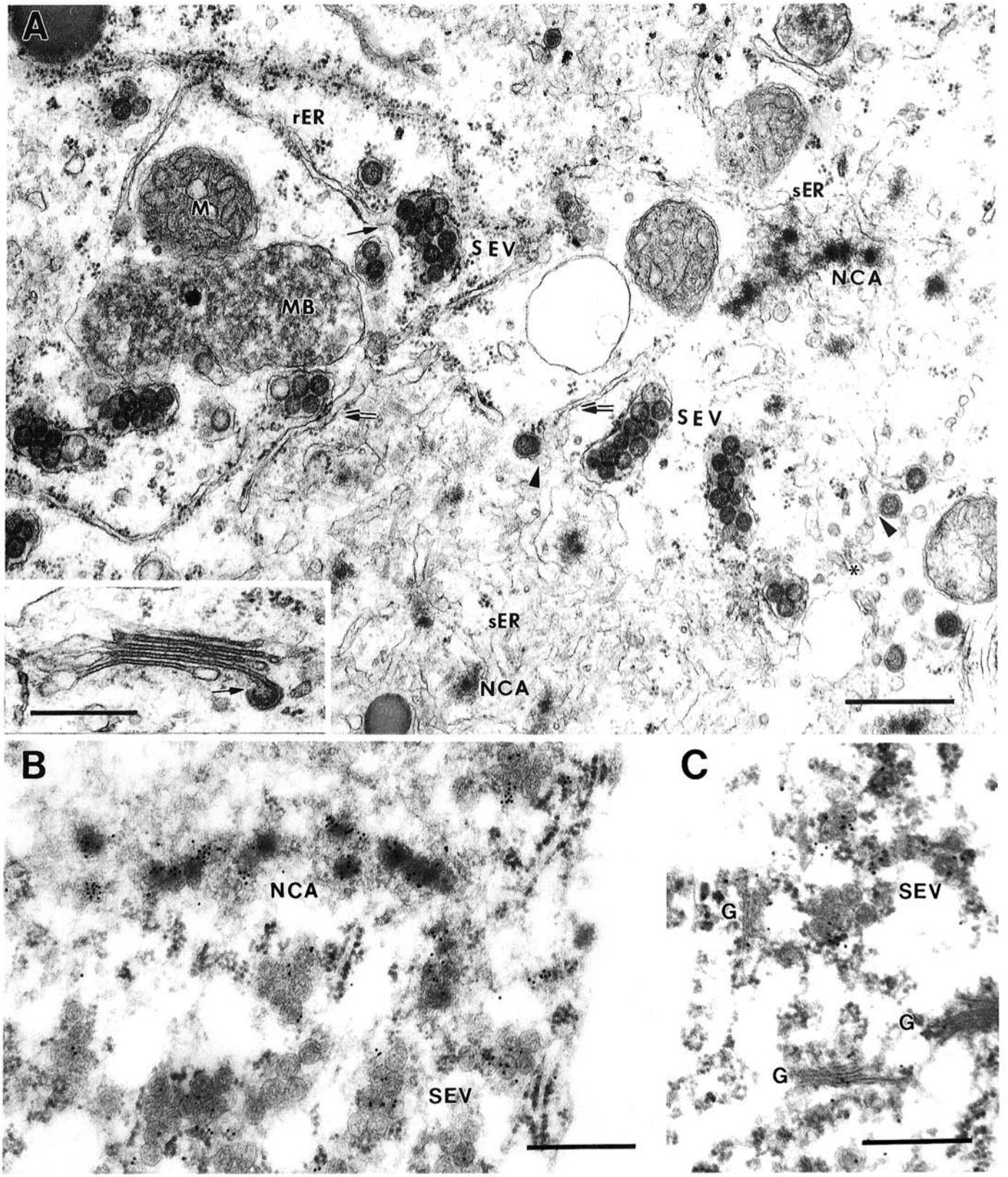


**Fig. 8.** Cytopathology of nondefective impatiens necrotic spot virus (INSV) isolate B in *Impatiens* 'Accent Salmon.' **A,** A nonnecrotic parenchyma cell containing extensive rough and smooth endoplasmic reticulum (rER and sER, respectively) and virions in different states of envelopment. Clustered single-enveloped virions (SEV) were present in ribosome-studded, swollen cisternae attached (arrow) to rER, whereas nucleocapsid aggregates (NCA) and double-enveloped virions (DEV) (arrowheads) were associated with sER. Smooth ER was continuous with rER (double arrows) and associated with tubular vesicles (asterisk). Budding occurred at Golgi bodies (inset). Bar = 510 nm. Bar, inset = 330 nm. **B,** Antibody to INSV nucleocapsid (N) protein reacted more strongly with NCA than with SEV in immunogold labeling tests. Bar = 250 nm. **C,** Three Golgi bodies (G) showing variability in labeling in immunogold labeling tests with antibody to INSV N protein. Bar = 250 nm.

tospovirus infections, except that PPMs typically appear as linear, oval, or curved structures (5,10,14) that are considerably smaller than the concentric membranes in Igg infections. When nucleocapsids bud through PPMs, they are thought to be enveloped by double membranes and result in DEVs (14). The significance of membrane proliferation in Igg-infected cells is unclear, but if these formations are analogous to PPMs, they may be manifestations of the defect in virion maturation.

The relationship between AIs and PPMs in Igg was unclear because AIs were usually located within areas of membrane proliferation but not between concentric PPMs. In thrips, AI produced by TSWV have been identified as G protein by immunogold labeling (18), but in plants, their identity has not been established. Because antiserum to G protein was not available during the course of this study, localization of G protein was not undertaken. Preliminary results from labeling tests with a monoclonal antibody to G1 protein have not revealed the presence of G1 protein in amorphous inclusions, however.

HT-1 appeared quite different from the other three isolates, both in the serological reactivity of the N protein and in the unusual heterogeneous mixture of viral structures and host membrane modifications induced in infections. Since this study was performed, preliminary information became available indicating that HT-1 is a member of tospovirus serogroup IV. Polyclonal antisera to HT-1 N protein reacted with serogroup IV isolate watermelon silver mottle virus in Western blots (S. D. Yeh, *personal communication*), and monoclonal antibodies to HT-1 N protein reacted in ELISA exclusively with serogroup IV isolates (G. Adam, *personal communication*). It is unknown whether the unusual structural features observed in HT-1 infections are characteristic of other serogroup IV isolates.

The cytopathological differences between HT-1 and the other three isolates were related to the appearance of PPMs, virions, and N protein accumulations and to modifications of host membranes. PPMs were ubiquitous in mature HT-1 infections, despite the fact that PPMs are typically transitory structures in tospovirus infections (5,14). There was considerable variability in structure, with linear, circular, and horseshoe forms observed. Electron-dense material accumulating around PPMs and Golgi bodies was labeled with antiserum to HT-1 N protein in immunogold labeling tests, verifying that this is nucleocapsid material and providing evidence supporting earlier reports that tospovirus particles form at these sites (10). Unusually large amounts of nucleocapsid material accumulated compared to other tospovirus infections (5,7, 10,14); this may be another manifestation of the defect in HT-1.

Budding profiles at Golgi bodies and PPMs in HT-1 infections resembled those of other tospoviruses, but many of the virions differed. Many cytoplasmic virions had only a single envelope, whereas many cisternal virions consisted only of electron-dense smears of irregular outline and shape. Furthermore, cisternal virion-like particles remained in rows within sER, failing to resolve into the clusters within swollen rER cisternae that are characteristic of many mature tospoviruses (5,7,9,10,14).

Another unusual feature of HT-1 infections was the low reactivity between HT-1 antiserum and cytoplasmic or cisternal virions and virion-like particles. The relatively low labeling may indicate that N protein is reduced, incomplete, or absent, N protein is present but is not that of HT-1, or HT-1 N protein is present and complete but modified so reactive antigenic sites are not exposed due to protein folding. The significance of the low serological reaction was not resolved in this study. Cytopathological features, however, were present to support further examination of this question. Although it seems unlikely that particles lack N protein entirely, their abnormal appearance is consistent with the conclusion that virion-like particles in HT-1 infections are incompletely formed or packaged. A second possibility, that N protein in particles is not that of HT-1, is supported by the range of inclusions in HT-1 infections that resemble nucleocapsid material but fail to label. A third possibility, that HT-1 N protein is present in virion-like particles but with hidden antigenic sites, is supported by the presence of HT-1 N protein at budding sites where virions are produced.

Unlike HT-1 infections, those of INSV HT-2 usually appeared to have progressed beyond the budding stage, and budding profiles were rare. Although HT-2 infections contained SEVs clustered in the rER, high populations of DEVs also were present and were often associated with the sER. Because some HT-2 virions matured while others did not, HT-2 infections may contain mixed populations of partially defective and nondefective virions. Many DEVs may be inherently unstable. Cytoplasm contained numerous structures resembling incomplete virions, many retaining evidence of a double membrane.

HT-2 occasionally and the nondefective isolate INSV B routinely produced virions characteristic of many mature tospovirus infections; these were associated with the rER not the sER. The sER, however, appeared to play a prominent role not previously reported in tospovirus infections. In HT-1, HT-2, and B infections, virions were found in tubular cisternae resembling segments of sER as well as in extensive cisternal labyrinths that were more clearly identified as sER networks. Although morphogenesis may occur by more than one pathway, we speculate that at least one pathway exists in which tubular sER-like cisternae containing SEVs represent an intermediate step. Time-course studies are necessary to determine if DEVs bud from or fuse to sER or if both occur.

The importance of sER apparently extends beyond a transitional structure. In cells containing SEVs in rER, prominent sER networks were present and relatively free of virions. In higher plants, sER is usually not well developed except in specialized cells where it may be associated with secretion and transport of lipophilic substances and glycogen (2,16). Smooth ER is generally thought to originate from the rER (2), but in HT-1, HT-2, and B infections, Golgi vesicles apparently contributed to expanding membrane surfaces. Fusion of Golgi vesicles with ER cisternae during virion maturation has been proposed previously by Kitajima et al. (10) who suggested that Golgi vesicles carry G protein on their membranes, which fuse to and are incorporated into the ER. Nucleocapsids, thus, would acquire envelopes with G proteins when they budded through ER membranes to become SEVs. In this study, although there appeared to be a close physical association between sER and NCA, budding was not seen through either sER or rER. Budding may occur, however, at a time in the infection cycle that was not observed. Although one function of the sER network may be to provide membranes for budding nucleocapsids, alternative or additional functions may relate more closely to those of the sER itself.

Because Igg, HT-1, HT-2, and B each appeared to reach a different stage of maturation, the four isolates may serve as valuable reference points in investigations of the replication cycle of INSV. Time-course studies of infections caused by the four isolates have been initiated to examine the infection process in greater detail.

## LITERATURE CITED


1. Bishop, D. H. L., Calisher, C. H., Casals, J., Chumakov, M. P., Gaidamovich, S. Y., Hannoun, C., Lvov, D. K., Marshall, I. D., Oker-Blom, N., Pettersson, R. F., Porterfield, J. S., Russell, P. K., Shope, R. E., and Westaway, E. G. 1980. Bunyaviridae. Intervirology 14:125-143.
2. Chrispeels, M. J. 1980. The endoplasmic reticulum. Pages 389-412 in: The Biochemistry of Plants: A Comprehensive Treatise. Vol. 1, The Plant Cell. N. E. Tolbert, ed. Academic Press, New York.
3. de Haan, P., Kormelink, R., Peters, D., and Goldbach, R. 1990. Genetic organization and expression of the tomato spotted wilt virus genome. Pages 60-66 in: Virus-Thrips-Plant Interactions of Tomato Spotted Wilt Virus. Proc. USDA Workshop. USDA, ARS, ARS-87.
4. Francki, R. I. B., and Grivell, C. J. 1970. An electron microscope study of the distribution of tomato spotted wilt virus in systemically infected *Datura stramonium* leaves. Virology 42:969-978.
5. Francki, R. I. B., Milne, R. G., and Hatta, T. 1985. Tomato spotted wilt

virus group. Pages 101-110 in: Atlas of Plant Viruses. Vol. 1. CRC Press, Boca Raton, FL.
6. German, T. L., Ullman, D. E., and Moyer, J. W. 1992. Tospoviruses: Diagnosis, molecular biology, phylogeny, and vector relationships. Annu. Rev. Phytopathol. 30:315-348.
7. Ie, T. S. 1971. Electron microscopy of developmental stages of tomato spotted wilt virus in plant cells. Virology 43:468-479.
8. Ie, T. S. 1982. A sap-transmissible, defective form of tomato spotted wilt virus. J. Gen. Virol. 59:387-391.
9. Kitajima, E. W. 1965. Electron microscopy of Vira-Cabeca virus (Brazilian tomato spotted wilt virus) within the host cell. Virology 26:89-99.
10. Kitajima, E. W., de Avila, A. C., Resende, R. de O., Goldbach, R. W., and Peters, D. 1992. Comparative cytological and immunological labeling studies on different isolates of tomato spotted wilt virus. J. Submicrosc. Cytol. Pathol. 24:1-14.
11. Kormelink, R. J. M. 1994. Structure and expression of the tomato spotted wilt virus genome, a plant-infecting bunyavirus. Ph.D. thesis. Agricultural University of Wageningen, Wageningen, Netherlands.
12. Law, M. D., and Moyer, J. W. 1990. A tomato spotted wilt-like virus with a serologically distinct N protein. J. Gen. Virol. 71:933-938.
13. Lawson, R. H., Dienelt, M. M., and Hsu, H. T. 1993. Effects of passaging a defective isolate of impatiens necrotic spot virus at different temperatures. Phytopathology 83:662-670.
14. Milne, R. G. 1970. An electron microscope study of tomato spotted wilt virus in sections of infected cells and in negative stain preparations. J. Gen. Virol. 6:267-276.
15. Milne, R. G., and Francki, R. I. B. 1984. Should tomato spotted wilt virus be considered as a possible member of the family *Bunyaviridae*? Intervirology 22:72-76.
16. Newcomb, E. H. 1980. The General Cell. Pages 2-50 in: The Biochemistry of Plants: A Comprehensive Treatise. Vol. 1, The Plant Cell. N. E. Tolbert, ed. Academic Press, New York.
17. Resende, R. de O., de Haan, P., de Avila, A. C., Kitajima, E. W., Kormelink, R., Goldbach, R., and Peters, D. 1991. Generation of enveloped and defective interfering RNA mutants to tomato spotted wilt virus by mechanical passage. J. Gen. Virol. 72:2375-2383.
18. Ullman, D. E., Sherwood, J. L., German, T. L., Westcot, D. M., Chenault, K. D., and Cantone, F. A. 1993. Location and composition of cytoplasmic inclusions in thrips cells infected with tomato spotted wilt virus. (Abstr.) Phytopathology 83:1374.
19. Urban, L. A., Huang, P.-Y., and Moyer, J. W. 1991. Cytoplasmic inclusions in cells infected with isolates of L and I serogroups of tomato spotted wilt virus. Phytopathology 81:525-529.
20. Vaira, A. M., Roggero, P., Luisoni, E., Masenja, V., Milne, R. G., and Lisa, V. 1993. Characterization of two tospoviruses in Italy: Tomato spotted wilt and impatiens necrotic spot. Plant Pathol. 42:530-542.
21. Verkleij, F. J., and Peters, D. 1983. Characterization of a defective form of tomato spotted wilt virus. J. Gen. Virol. 64:677-686.